electronics

MDPI

Article

Neural-Network-Based Interference Cancellation for MRC and EGC Receivers in Large Intelligent Surfaces for 6G

Mário Marques da Silva [1,2,3,4,*], Gelson Pembele [5] and Rui Dinis [2,3,5]

[1] Department of Engineering and Computer Sciences, Universidade Autónoma de Lisboa, 1169-023 Lisboa, Portugal
[2] Autonoma TechLab, 1169-023 Lisboa, Portugal
[3] Instituto de Telecomunicações, 1049-001 Lisboa, Portugal
[4] Ci2—Centro de Investigação em Cidades Inteligentes, 2300-313 Tomar, Portugal
[5] Faculty of Sciences and Technology, Universidade Nova, 2829-516 Caparica, Portugal; gpembele@autonoma.pt
* Correspondence: mmsilva@autonoma.pt

Abstract: Large Intelligent Surfaces (LISs) have emerged as a promising technology for enhancing spectral efficiency and communication capacity in the Sixth Generation of Cellular Communications (6G). Low-complexity receiver architectures for LISs rely on Maximum Ratio Combining (MRC) and Equal Gain Combining (EGC) receivers, often complemented by iterative detection techniques for interference mitigation. In this work, we propose a novel approach where a neural network replaces iterative interference cancellation, learning to estimate the transmitted signals directly from the received data, mitigating interference without requiring iterative cancellation. Moreover, this also eliminates the need for channel matrix inversion at each frequency component, as required for Zero Forcing (ZF) and Minimum Mean Squared Error (MMSE) receivers, reducing computational complexity while still achieving a good performance improvement. The neural network parameters are optimized to balance performance and computational cost.

Keywords: LIS systems; 6G; receiver types; neural networks

Academic Editors: Soo Young Shin and Muneeb Ahmad

Received: 12 April 2025
Revised: 16 May 2025
Accepted: 19 May 2025
Published: 21 May 2025

Citation: Marques da Silva, M.; Pembele, G.; Dinis, R. Neural-Network-Based Interference Cancellation for MRC and EGC Receivers in Large Intelligent Surfaces for 6G. *Electronics* **2025**, *14*, 2083. https://doi.org/10.3390/electronics14102083

1. Introduction

The Fourth Industrial Revolution, also known as Industry 4.0, focuses on optimizing resources while integrating advanced human skills. It is characterized by the increasing use of robotics, artificial intelligence (AI), the Internet of Things (IoT), and big data, which, together, are transforming industries, services, and daily life [1]. A key aspect of this revolution is the replacement of human labor with machines or the enhanced interaction between the two [2]. Similar to past industrial revolutions, Industry 4.0 seeks to improve efficiency in resource utilization. Automation is a prime example, enabling, e.g., the development of autonomous vehicles and accelerating the adoption of car-sharing by removing the need for human drivers.

A major technological enabler of Industry 4.0 is the evolution of mobile communications, particularly the transition from fifth-generation (5G) to sixth-generation (6G) systems. While 5G enabled direct machine-to-machine communication [3], 6G aims to advance these capabilities with real-time data exchange, ultra-reliable low-latency communication, and high-speed connectivity for industrial automation and IoT applications. These developments are critical for applications like autonomous systems, remote healthcare, and smart infrastructure.

The upcoming 6G will further extend these capabilities by enabling advanced services such as holographic communication, immersive extended reality (XR), and next-generation autonomous systems. Additionally, 6G will facilitate seamless interaction with high-speed unmanned aerial vehicles, further expanding its impact across multiple sectors. To support these applications, 6G must achieve ultra-high data rates, an increased spectral efficiency, and minimal latency. Among the key enabling technologies, Large Intelligent Surfaces (LISs) stand out as a promising approach to improving spectral efficiency and communication reliability through large-scale antenna arrays.

To meet the demands of these new applications, 6G will need to achieve speeds of up to 1 terabit per second, substantially increase network capacity to support a higher density of connected devices, and dramatically reduce latency. These improvements are essential for real-time applications such as autonomous driving, online gaming, and the remote control of critical infrastructure. To enable such high-performance connectivity, 6G will rely on cutting-edge technologies, including block transmission techniques, advanced error correction codes, and LISs. The LIS concept represents an evolution beyond massive multiple-input multiple-output (MIMO) systems, incorporating an even larger number of antenna elements to enhance spectral efficiency and data transmission rates.

By integrating these innovations, 6G will provide the necessary foundation to interconnect billions of IoT devices with an unprecedented speed, reliability, and efficiency, driving the next phase of industrial and technological advancement.

The concept of LISs has gained significant attention as a means of improving wireless communication efficiency through large-scale antenna arrays. Unlike conventional MIMO systems, LISs exploit a dense array of antennas spread over an extended area, enabling enhanced beamforming and spatial multiplexing.

Wireless communications are typically established beyond the Fraunhofer distance, meaning that they operate in the far field [4]. While individual antenna elements of an LIS function in the far field, the LIS, as a whole, operates in the near field [4–7]. As a result, it can be considered a near-field beamformer, distinct from conventional beamformers in that it not only directs beams along azimuth and elevation angles, but also adjusts them based on distance. This latter capability (directing the beam through distance) helps to mitigate interference between users who share the same bearing and elevation but are positioned at different distances. It is worth noting that adjacent LIS antenna elements are usually spaced at $\lambda/2$, and the channel correlation between them enables the formation of the described beam.

It is worth noting that, as defined in [8], Reconfigurable Intelligent Surfaces (RISs) are another emerging technology closely related to LISs. While LISs typically involve active antenna elements with signal processing capabilities, RISs are usually passive or semi-passive structures that reflect incident signals by controlling their phase shifts, without active transmission. Both architectures face common challenges, particularly regarding channel estimation with large-scale surfaces and hardware constraints in millimeter wave communications and terahertz environments. Recent works on RIS-assisted systems, such as [9,10], have proposed parametric and two-stage estimation techniques to address these issues. The neural-network-based approach we propose for LISs could also inspire future research on RIS-related receiver strategies.

In LISs, the use of a large number of receiving antennas allows for a better spatial resolution and increased diversity, enabling the system to distinguish and recover multiple transmitted signals more effectively. Traditional receivers such as MRC (Maximum Ratio Combining), EGC (Equal Gain Combining), Zero-Forcing (ZF), and MMSE (Minimum Mean Squared Error) have been widely studied and applied due to their mathematical tractability and relatively low complexity [7,11,12]. However, these methods are often

limited by assumptions such as perfect channel state information and the linearity of the channel model. Moreover, solutions based on matrix inversion—such as ZF and MMSE—can become computationally expensive when scaling to a large number of antennas [7,12].

A key challenge in LIS-based communication systems is multi-user interference (MUI), which significantly impacts system performance. Receivers, such as MRC and EGC, generate interference in the decoding process, which tends to degrade performance. Contrarily, ZF and MMSE receivers do not generate interference in the decoding process, but they require matrix inversion, leading to computational challenges.

In contrast, deep learning approaches offer the possibility of learning implicit representations of the channel and estimating the transmitted symbols directly from the received signals, without requiring an explicit inversion of the channel matrix. Recent advances have demonstrated the potential of deep learning to replace traditional detection and equalization techniques in communication systems, either by training detection algorithms without any prior knowledge of the channel model [13] or by jointly learning equalization and decoding processes to improve performance in non-linear and dispersive channels [14]. This opens the door to more robust and potentially lower-complexity receiver architectures, especially when optimized for specific environments or channel conditions. In particular, deep-learning-based receivers can adapt to complex propagation scenarios, non-linearities, and hardware impairments and may be trained to outperform traditional linear techniques under certain conditions.

The motivation of this work is, thus, to investigate whether a neural-network-based receiver can provide a viable alternative to conventional receivers, especially MRC and EGC, which are attractive for their simplicity, in the context of LIS systems. This includes evaluating whether a deep neural network can implicitly learn to perform the same role as these techniques (or better) while maintaining a low computational complexity and reducing the reliance on analytical channel models.

In this work, we investigate an LIS system [11,12,15–17] employing single-carrier transmission with frequency-domain equalization (SC-FDE) [18,19], which serves as an alternative to orthogonal frequency division multiplexing (OFDM). Since OFDM signals typically exhibit a high peak-to-average power ratio (PAPR), their use in uplink scenarios tends to be less efficient. In contrast, SC-FDE features a lower PAPR, making it a more appropriate choice for uplink communications. This paper evaluates the performance of four different receivers—ZF, MMSE, MRC, and EGC [20,21]—providing a comparative analysis of their effectiveness.

The contributions of this work are as follows:

- We propose a neural-network-based interference cancellation approach for LISs, eliminating the need for the iterative decoding traditionally used with MRC/EGC receivers.
- We demonstrate that MRC and EGC receivers enhanced with neural networks outperform conventional ZF/MMSE receivers or MRC/EGC with iterative interference suppression, achieving a better balance between computational efficiency and performance.
- We show that our method avoids the need for channel matrix inversion, reducing computational complexity while maintaining a competitive performance.

The structure of this paper is organized as follows: Section 2 describes the system and signal models; Section 3 introduces the neural-network-based interference cancellation approach; Section 4 presents and analyzes the performance results; and Section 5 concludes the paper.

2. System and Signal Characterization

The evolution of 6G communications is anticipated to meet stringent performance requirements, including a peak data rate of at least 1 Tbps for nomadic access—100 times greater than 5G—and 1 Gbps in mobile scenarios, which is 10 times higher than its predecessor. Additionally, energy efficiency is projected to improve by a factor of 10 to 100, while spectral efficiency is expected to be enhanced by 5 to 10 times in comparison to 5G. These advancements are expected to be realized through the implementation of LISs operating in the terahertz spectrum, combined with block transmission techniques. It is important to note that increasing the carrier frequency results in a larger channel coherence bandwidth, translated into a higher throughput.

LIS technology is particularly compatible with terahertz frequencies due to the reduced wavelength, which enables the use of ultra-compact antennas, thereby simplifying the deployment of cost-effective LIS panels. However, as the number of antennas in an LIS grows—effectively functioning as a beyond-massive MIMO system—the associated signal processing demands also increase significantly. Consequently, there is a crucial need to explore receiver architectures with minimal complexity. This study links low-complexity receivers, which streamline the decoding process, aiming to optimize performance while keeping the computational complexity acceptable.

To mitigate intersymbol interference, block transmission techniques are frequently employed. The SC-FDE method, in particular, offers the following key advantage over OFDM: it exhibits a lower PAPR [18,19]. This characteristic makes it especially suitable for uplink scenarios and enhances the efficiency of power amplification [22].

Unlike conventional communications between user equipment (UE) and a base station (BS), LIS-based communication typically relies on line-of-sight connectivity. The LIS functions as a short-range beamformer, with antenna elements spaced at half-wavelength intervals—much shorter than the three to four wavelengths commonly used in traditional MIMO configurations. While individual LIS antenna elements communicate in the far field, the overall LIS array operates within the near field, meaning that communication occurs at distances shorter than the Fraunhofer limit, typically spanning just a few wavelengths. This unique property gives LISs distinctive capabilities. Whereas conventional beamforming is confined to azimuth and elevation adjustments, LISs extend this capability to the distance dimension as well. This enables interference mitigation from users who are aligned in azimuth and elevation but are positioned at varying distances.

Focusing on Figure 1, the nth transmitted block—comprising N data symbols—from the tth UE is denoted as $s_n^{(t)}$, while the received block received by the rth antenna of the LIS is denoted as $y_n^{(r)}$. The relationship between the time-domain and the frequency-domain signals for the kth subcarrier (assuming that they remain constant throughout the transmission of a given block) is established via the Discrete Fourier Transform (DFT), such that $DFT\left\{s_n^{(t)}; n = 0, 1, \ldots, N-1\right\} = \left\{S_k^{(t)}; k = 0, 1, \ldots, N-1\right\}$, i.e., the DFT is applied to the time-domain block. The same procedure, mutatis mutandis, is applied to the received signal block, channel, and noise.

The received signal in the frequency domain, expressed in matrix–vector form, is given by [22], as follows:

$$\mathbf{Y}_\mathrm{k} = \left[Y_k^{(1)}, \ldots, Y_k^{(R)}\right] = \mathbf{H}_\mathrm{k}\mathbf{S}_\mathrm{k} + \mathbf{N}_\mathbf{k}. \tag{1}$$

Here, $\mathbf{Y}_k$ is the R-dimensional received vector at subcarrier k, $\mathbf{S}_k$ is the T-dimensional transmitted signal vector, $\mathbf{H}_k$ is the R $\times$ T channel matrix whose (r, t)-th element is denoted as $H_k^{(t,r)}$, and $\boldsymbol{N_k}$ is the R-dimensional noise vector for the subcarrier [22].

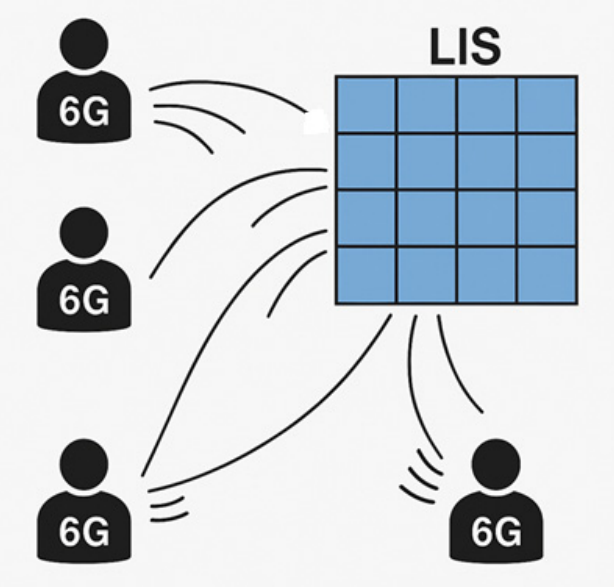

Figure 1. An LIS serving four 6G users.

Receiver System and Signal Modeling

It is well-established that ZF and MMSE receivers are computationally intensive, as they require channel inversion for each frequency component, which results in significant battery consumption. ZF receivers offer the benefit of effectively mitigating intersymbol interference. However, they also suffer from increased noise levels under moderate to high noise conditions, leading to a degradation in performance. In contrast, MRC and EGC receivers avoid such complexity, resulting in a simpler receiver architecture that is particularly advantageous in LIS scenarios with a very large number of antenna elements. However, MRC and EGC receivers introduce some interference during the decoding process, which can be mitigated using iterative receivers.

Considering a non-iterative receiver, the estimated frequency domain data symbols $\tilde{\mathbf{S}}_k = \left[\tilde{S}_k^{(1)}, \ldots, \tilde{S}_k^{(R)}\right]^T$ are defined as follows:

$$\tilde{\mathbf{S}}_k = \boldsymbol{B}_k^H \boldsymbol{Y}_k. \tag{2}$$

Depending on the algorithm, $\mathbf{B}_k$ can be computed differently [20]. Using a ZF receiver, $\mathbf{B}_k$ becomes $\mathbf{B}_k = \mathbf{H}_k^H \left(\mathbf{H}_k \mathbf{H}_k^H\right)^{-1}$, while $\mathbf{B}_k$ becomes $\mathbf{B}_k = \left(\mathbf{H}_k \mathbf{H}_k^H + \beta \mathbf{I}\right)^{-1} \mathbf{H}_k^H$ for the MMSE, where $\beta = \frac{\sigma_N^2}{\sigma_S^2} = \frac{\frac{E\left[|N_k|^2\right]}{2}}{\frac{E\left[|S_k|^2\right]}{2}}$ and where $\mathbf{I}$ is an $R \times R$ identity matrix. Using the MRC receiver, $\mathbf{B}_k$ becomes $\mathbf{B}_k = \mathbf{H}_k^H$ and $\mathbf{B}_k$ becomes $\mathbf{B}_k = exp\left\{j\, arg\left(\mathbf{H}_k^H\right)\right\}$ for the EGC.

Iterative block decision feedback equalization (IB-DFE) [19] is a highly efficient receiver for SC-FDE, utilizing feedforward and feedback coefficients for an enhanced performance. While MRC and EGC are computationally simple, they generate residual interference, especially with moderate signal-to-noise ratio (SNR) values. This can be countered by iterative receivers, similar to IB-DFE, implementing the following function:

$$\tilde{\mathbf{S}}_k = \mathbf{B}_k^H \mathbf{Y}_k - \mathbf{C}_k \bar{\mathbf{S}}_k \tag{3}$$

where the interference cancellation matrix, $\mathbf{C}_k$, is computed as $\mathbf{C}_k = \mathbf{A}_k^H \mathbf{H}_k - \mathbf{I}$ [21], and $\mathbf{I}$ is an $R \times R$ identity matrix.

As an alternative to this iterative receiver, we propose an interference cancellation process applied at the output of the MRC/EGC receiver (with a single iteration), based on a neural network, as defined in the following.

3. Neural-Network-Based Interference Cancellation in LIS Systems

In this work, we propose a neural-network-based approach for interference cancellation in LISs, specifically targeting MRC and EGC receivers. Traditional iterative interference cancellation methods are sub-optimal [7]. On the other hand, when using ZF or MMSE receivers, significant computational complexity is required due to the repeated matrix inversions required at each channel frequency component. Our approach leverages neural networks to learn a mapping from received signals to transmitted signals, effectively bypassing the need for iterative interference cancellation. The neural network is trained to learn the relationship between the received signal, which is affected by interference, and the transmitted signal, represented by $\mathbf{S}_k$. This allows the network to remove the interference without the need for direct channel matrix inversion or an iterative receiver.

3.1. Neural Network Architecture

The neural network model was designed considering the trade-off between computational complexity and performance improvement. Extensive testing showed that increasing the network depth beyond three fully connected layers did not lead to significant performance improvements, while a shallower network resulted in a degraded signal recovery. As such, the proposed architecture consists of three key fully connected layers, each serving a specific role in feature extraction and signal reconstruction.

The proposed Multi-Layer Perceptron (MLP) architecture is well-suited for interference cancellation in LISs using MRC/EGC due to its ability to learn non-linear mappings between the received signals and the transmitted signals. Since interference is generated during the decoding process rather than being a direct function of the channel matrix inversion, the primary goal is to estimate and remove this interference rather than reconstruct the original transmitted signal through explicit channel equalization. The MLP effectively captures the complex signal relationships introduced by MRC/EGC processing while maintaining a manageable computational cost. Other architectures, such as Convolutional Neural Networks (CNNs) and Long Short-Term Memory (LSTM) networks, were also evaluated but found to be less appropriate, as the interference structure lacks significant spatial or temporal correlations. Additionally, the structure of the MLP network, with three fully connected layers and ReLU activations, ensures a sufficient level of non-linearity to model the interference effects while avoiding unnecessary complexity that could lead to overfitting.

The aim of the neural network relies on removing interference (see Figure 2). To ensure robust learning, the dataset is structured such that each transmit antenna has a dedicated neural network trained independently. Note that the aim is to estimate the signals transmitted by each one of the transmit antennas. This design choice was motivated by the observation that training a single network for all antennas introduced inconsistencies due to the varying channel conditions across antennas. The choice to train independent networks for each antenna was based on the variability of channel conditions across antennas. This ensures that the network can adapt more accurately to the specific conditions of each antenna, resulting in more efficient signal reconstruction.

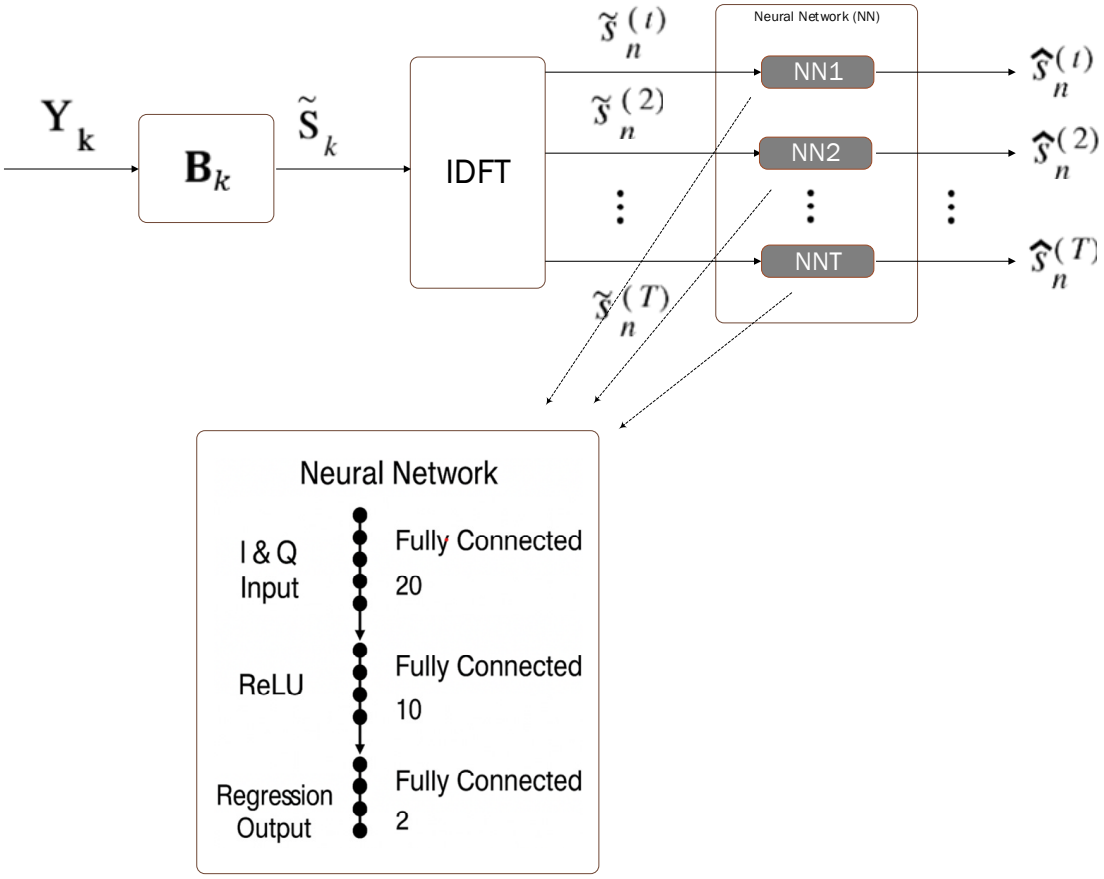

Figure 2. Block diagram of the MRC/EGC with neural receiver.

As inputs, the network receives the received signals at the output of the MRC/EGC detector $\tilde{S}_n^{(t)}$, corresponding to the estimation of the tth transmitted antenna, where the in-phase (I) and quadrature (Q) components are treated as separate features. Note that the neural network processes signals in the time domain. These two components (I and Q) are jointly fed to the network, in a new dimension of the matrix, to achieve the required correlation during training and prediction processes. The input to the neural network is structured as a two-dimensional vector, where the **I** and **Q** parts of the received signal are presented as separate features but concatenated to maintain correlation during training, as follows:

$$\tilde{S}_n^{(t)} = \begin{bmatrix} \mathfrak{R}(\tilde{S}_n^{(t)}) \\ \mathfrak{I}(\tilde{S}_n^{(t)}) \end{bmatrix} \tag{4}$$

The length of the dataset is N, the block size during training.
The architecture consists of the following layers:

- Feature Input Layer: A featureInputLayer with two input features (I and Q components), ensuring compatibility with the structure of complex-valued signals, compatible with QPSK (Quadrature Phase-Shift Keying) complex modulation.
- Fully Connected Layer 1: A fullyConnectedLayer with 20 neurons, responsible for the initial feature extraction.
- ReLU Activation: A reluLayer to introduce non-linearity, improving the network's ability to capture complex signal relationships.
- Fully Connected Layer 2: A fullyConnectedLayer with 10 neurons, further refining the extracted features.
- ReLU Activation: Another reluLayer to enhance non-linearity and robustness.

- Fully Connected Output Layer: A fullyConnectedLayer with two neurons, reconstructing the in-phase and quadrature components of the transmitted signal.
- Regression Output Layer: A regressionLayer to optimize the network for minimizing signal reconstruction errors.

This configuration was selected after an extensive evaluation of various network depths and neuron configurations. More complex architectures with additional layers and neurons did not provide significant performance improvements, while reducing the network's depth led to a noticeable degradation in signal reconstruction accuracy.

3.2. Training Process

The training data consist of received signals, detected by MRC/EGC with a single iteration, as inputs, with their corresponding transmitted signals as outputs. The output of the MRC/EGC decoder is corrupted by interferences generated in the decoding process (Equation (2)).

The training process minimizes the Mean Squared Error (MSE) between the predicted and actual transmitted signals, as follows:

$$\varsigma = \frac{1}{N}\sum_{n=1}^{N} \left|\left| \overset{\sim}{\mathrm{S}}_n^{(t)} - \hat{\mathrm{S}}_n^{(t)} \right|\right|^2 \tag{5}$$

where $\overset{\sim}{\mathbf{S}}_n^{(t)}$ is the actual output signal from the one-iteration MRC/EGC detector, while $\hat{\mathbf{S}}_n$ is the estimated output of the neural network (same signal clean of interference).

Training was performed using the Adam optimizer with the following hyperparameters:

- Max Epochs: 500
- Mini-Batch Size: 16
- Initial Learning Rate: 0.001
- Shuffling: Enabled at every epoch to prevent overfitting

Each neural network was trained to minimize the MSE between the predicted and actual transmitted signals. The batch size of 16 was chosen as a balance between training stability and convergence speed.

3.3. Inference and Signal Reconstruction

During inference, the trained neural networks estimate the transmitted signal from the received signal on a per-antenna basis. Given that each antenna has its own dedicated model, predictions are performed individually, ensuring optimal signal reconstruction for each channel condition.

For each received symbol, the I and Q components are extracted as $\hat{\mathrm{S}}_n^{(t)} = \begin{bmatrix} \mathfrak{R}\left(\hat{\mathrm{S}}_n^{(t)}\right) \\ \mathfrak{I}\left(\hat{\mathrm{S}}_n^{(t)}\right) \end{bmatrix}$, processed through the trained model, and recombined to form the following estimated complex-valued transmitted signal:

$$\hat{\mathrm{S}}_n^{(t)} = \mathrm{R}\left(\hat{\mathrm{S}}_{\mathrm{n}}^{(\mathrm{t})}\right) + j\mathfrak{I}\left(\hat{\mathrm{S}}_{\mathrm{n}}^{(\mathrm{t})}\right) \tag{6}$$

As follows, each layer in the neural network applies a transformation, where a fully connected layer follows:

$$\mathrm{z}^{(\mathrm{l})} = \max\left(0, \mathrm{W}^{(\mathrm{l})}\mathrm{z}^{(\mathrm{l}-1)} + \mathrm{b}^{(\mathrm{l})}\right) \tag{7}$$

where $\mathrm{W}^{(l)}$ and $\mathrm{b}^{(l)}$ are the weights and biases of layer l, and the activation function ReLU ensures non-linearity.

This approach eliminates the need for iterative matrix inversions, significantly reducing computational overhead while surpassing the performance of conventional iterative interference cancellation techniques. The neural network drastically reduces the need for repeated matrix inversions, which are computationally intensive or iterative receivers, making the system more efficient in terms of processing time and energy consumption.

In terms of computational complexity, ZF and MMSE receivers require matrix inversion for each frequency component, with a per-subcarrier complexity of approximately $O(T^3)$, where T is the number of transmit antennas. MRC and EGC receivers avoid inversion, with complexity $O(R)$ per subcarrier (where R is the number of receiver antennas), but often rely on iterative interference cancellation.

In the proposed approach, a separate neural network is trained for each transmit antenna. As such, the total training complexity scales as $O(T \cdot N \cdot L)$, where N is the number of training samples per antenna and L is the number of trainable parameters per network. Although training is computationally intensive, it is performed per coherence interval and can be parallelized across antennas. The inference complexity is significantly lower, scaling as $O(T \cdot L)$, which makes the method suitable for real-time execution once training is completed. Future work will investigate optimizations such as parameter sharing and online adaptation to reduce training overhead in highly dynamic scenarios.

It is worth noting that the training of the neural network assumes perfect channel knowledge for supervision. In practical deployments, channel estimation errors may lead to discrepancies between the training labels and the actual received signals, potentially degrading performance. However, neural networks have shown the potential to tolerate moderate levels of estimation noise, especially when trained with representative or augmented data that include such effects. Future work will explicitly study the impact of imperfect CSI and explore training strategies to enhance robustness to estimation errors.

4. Simulation Results and Analysis

This section analyzes the performance of the LIS in terms of bit error rate (BER) as a function of E_b/N_0, where E_b denotes the energy per transmitted bit and N_0 represents the one-sided noise power spectral density. The results are obtained via Monte Carlo simulations, using SC-FDE for block-based transmission.

In the simulations, user locations are randomly distributed within the environment. The propagation channel comprises the following five multipath components: one direct line-of-sight (LoS) path and four reflections from surrounding walls. The power of each component is determined based on propagation characteristics, including the total path length and reflection-induced attenuation.

The results are based on QPSK modulation and a block size of $N = 256$ symbols, with a comparable performance observed for other large values of N. Figure 3 illustrates the 3D spatial distribution of users and the placement of the LIS panels, offering insight into how users align with the panels. The simulation environment consists of four ceiling-mounted panels, each equipped with a varying number of antennas. For the sake of simplicity, this figure only shows direct paths, not reflected paths.

In addition to conventional iterative receivers based on MRC and EGC used to mitigate the interferences generated in the decoding process, this work explores the application of neural networks for interference cancellation during the decoding process. These networks are trained to mitigate interference effects and optimize signal recovery. The Monte Carlo simulations incorporate multiple user distributions, as the positions of users are randomly reselected in each run, ensuring statistical robustness in the analysis. The performances obtained with the different receiver types are analyzed in multiple scenarios with various numbers of users and different numbers of antennas.

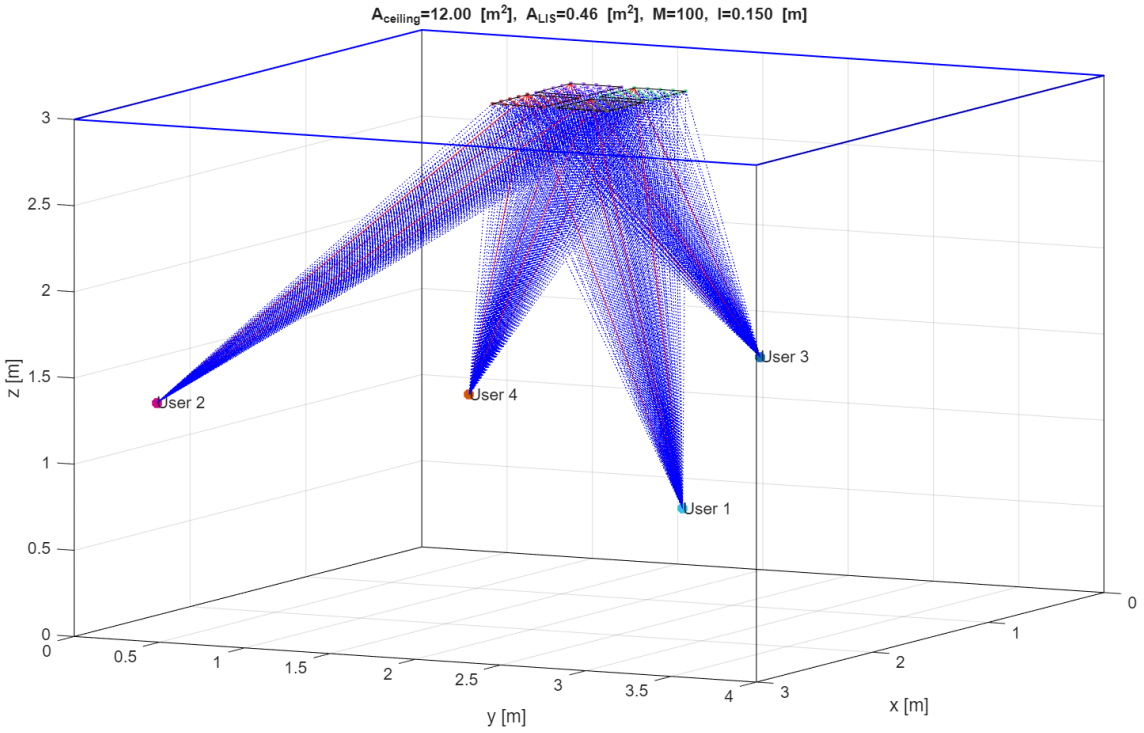

Figure 3. LIS scenario considered in the simulations with four panels on the ceiling (only direct paths are plotted).

Figure 4 presents the performance results for an LIS setup consisting of four panels, each equipped with 400 antennas, arranged in a 20 × 20 configuration per panel. This results in a total of 1600 antennas within the LIS. The scenario includes the following two users: one serving as the reference user and the other acting as an interfering user. As can be seen, the performance obtained with the MRC iterative receiver (five iterations) is approximately the same as that with ZF and MMSE receivers. Nevertheless, it is worth noting that ZF and MMSE receivers require the computation of the pseudo-inverse of the channel matrix for each frequency component of the channel, which is very computationally demanding. On the other hand, the EGC iterative receiver (five iterations) performs worse than MRC/ZF/MMSE. Observing the performance obtained with MRC and EGC associated with the neural network receiver, a performance improvement in the order of 5 dB, as compared with the corresponding iterative receiver, is clear. Note that the performances are even better than ZF and MMSE. It is viewed that the MRC neural receiver is the one that achieves the best overall performance, without requiring explicit channel matrix inversion. The neural network significantly minimizes the requirement for multiple matrix inversions, which are computationally demanding, enhancing the system's efficiency in both processing speed and energy usage. The training can be computationally demanding, but the prediction is straightforward. In contrast to conventional approaches, the neural network offers a more resource-efficient alternative while maintaining a high level of accuracy in signal estimation.

These results demonstrate that leveraging neural networks in LIS receivers provides a promising alternative to conventional interference cancellation techniques, paving the way for efficient and scalable implementations in future 6G communication systems.

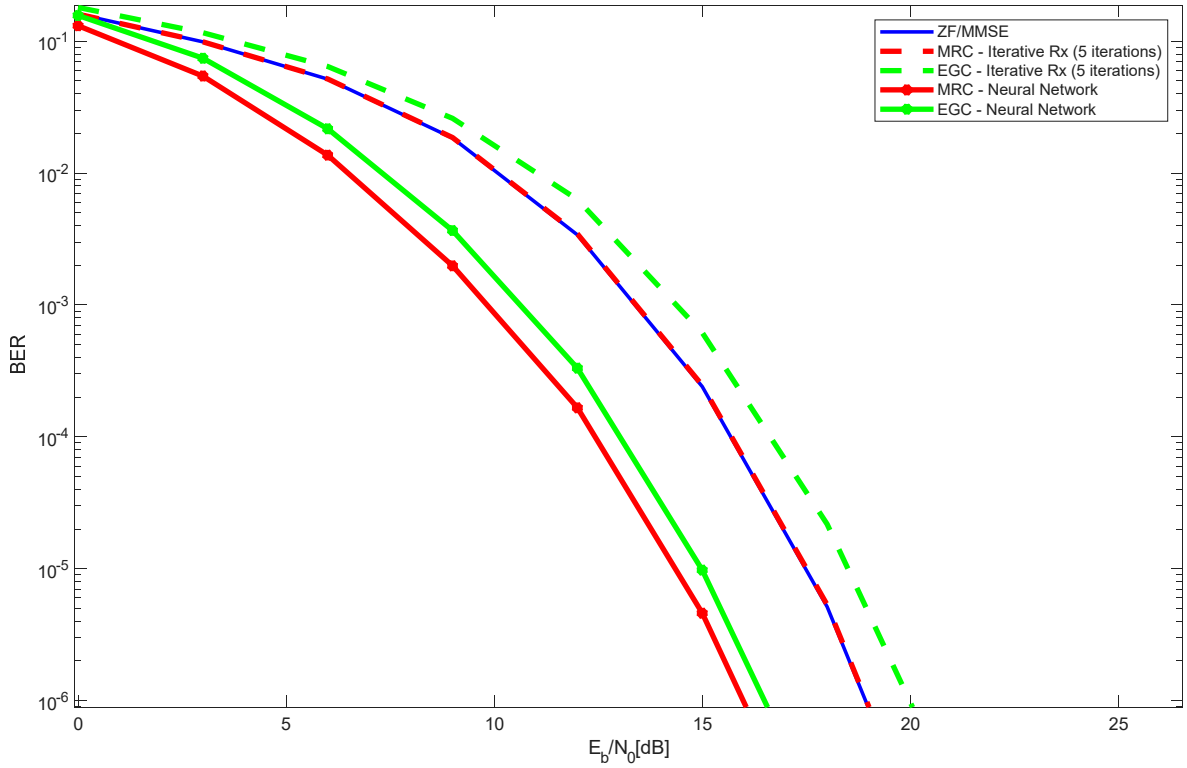

Figure 4. Performance results of the 4 × 400 LIS, with 2 users, with different receiver types.

Figure 5 illustrates the performance results for a 4 × 225 LIS configuration, considering two users and various receiver types. This setup consists of four panels, each containing 225 antennas, arranged in a 15 × 15 grid per panel, leading to a total of 900 antennas in the LIS. Similar to the previous figure, the scenario involves one reference user and one interfering user. The results indicate that, as observed earlier, the combination of MRC and EGC with a neural receiver outperforms iterative receivers, as well as ZF and MMSE methods. Among these, MRC with a neural receiver demonstrates the best performance, followed by EGC with a neural receiver, which still surpasses the results obtained with the ZF and MMSE techniques.

Figure 6 shows the performances of the following two LIS configurations: 4 × 400 and 4 × 225. Two users were considered in the simulations. As expected, the results obtained with 4 × 400 LIS configuration were always better than those obtained with 4 × 225 for all different receiver types. Moreover, it is observed that the best overall performance was obtained with the 4 × 400 LIS configuration and MRC neural receiver.

Figure 7 shows the performance results of the 4 × 400 LIS configuration, with 16 users, with an iterative receiver and with a neural network, for both MRC and EGC. The results for ZF/MMSE are also plotted. Similar to the observations in Figure 4 (with two users), Figure 7 demonstrates that, for a scenario with 16 users and the given LIS configuration, the MRC neural network receiver achieves the best overall performance. As expected, the performance of ZF/MMSE stays within that of MRC/EGC iterative receivers and MRC/EGC neural network receivers.

Figure 8 presents the performance results for the 4 × 4004 LIS configuration with varying numbers of users (2, 8, and 16), using both iterative and neural-network-based receivers, for MRC and EGC schemes. The results for ZF and MMSE receivers are also included. As expected, the performance declines as the number of users increases. However, the degradation observed when increasing from 8 to 16 users is minimal. This occurs because the LIS is able to mitigate interference very efficiently. The receiver that achieves

the best overall performance, regardless of the number of users, is the MRC with the neural network receiver, followed by EGC.

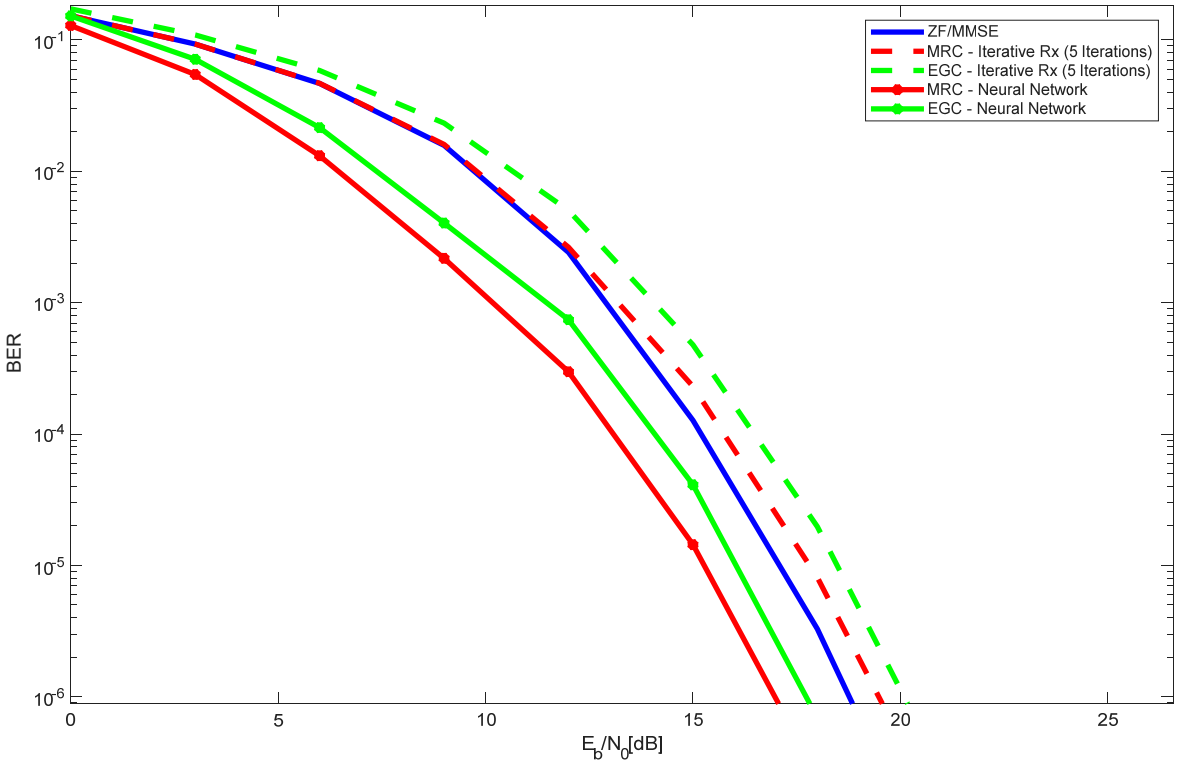

Figure 5. Performance results of the 4 × 225 LIS, with 2 users, with different receiver types.

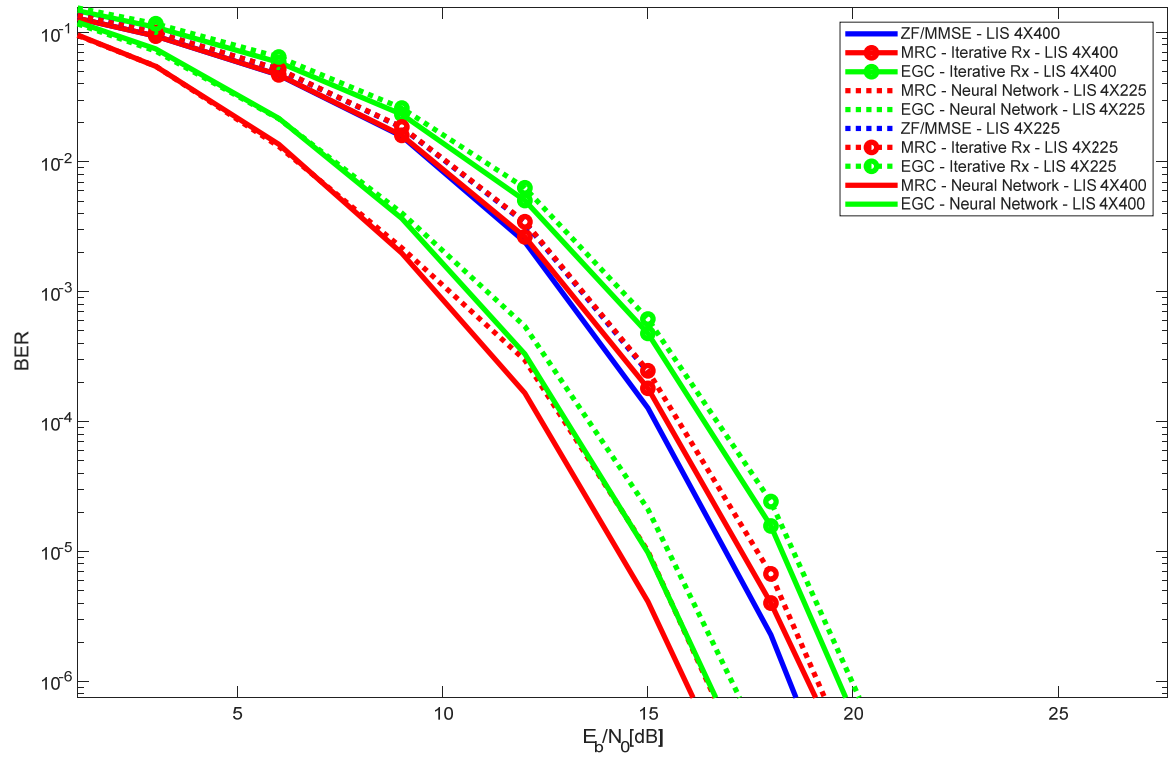

Figure 6. Performance results of several LIS configurations, with 2 users, and different receiver types.

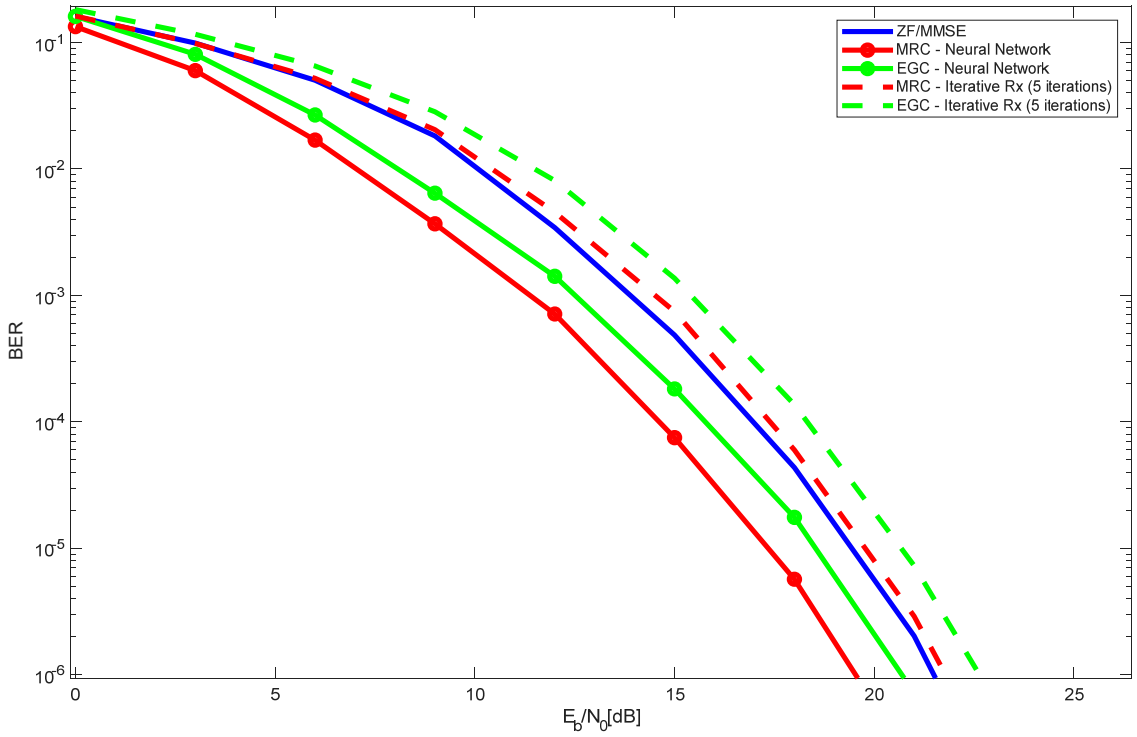

Figure 7. Performance results of the 4 × 400 LIS, with 16 users, with different receiver types.

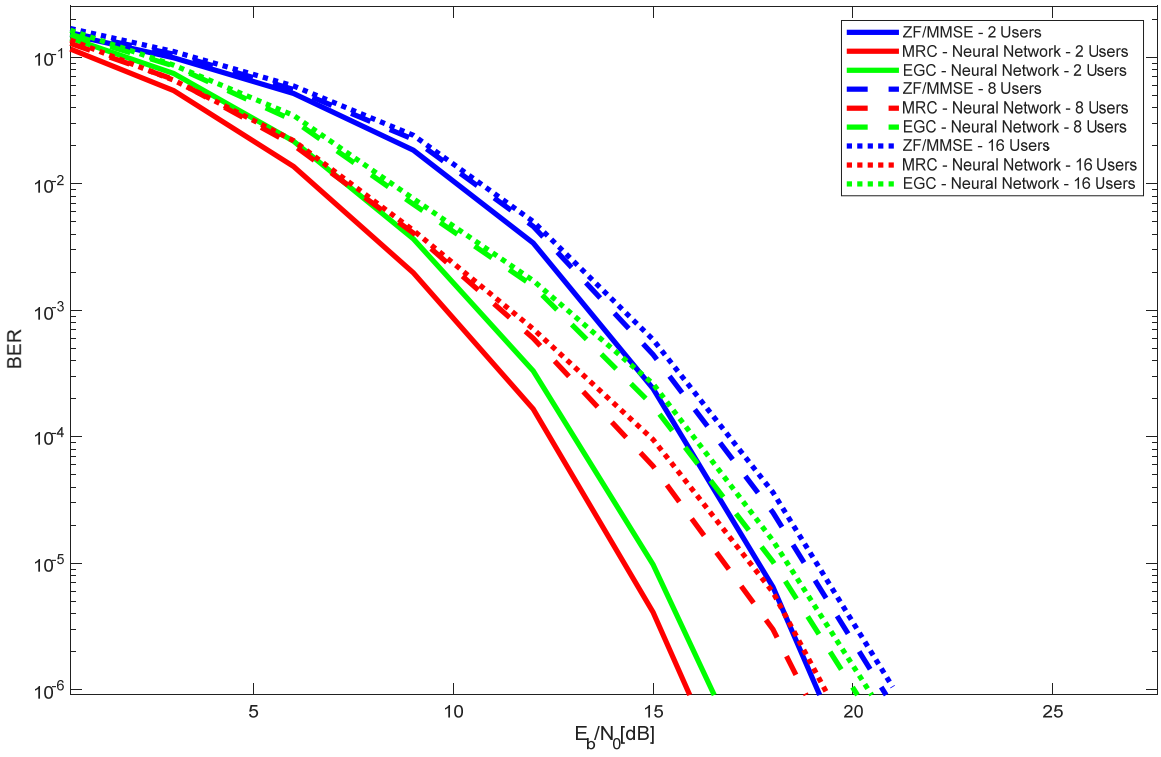

Figure 8. Performance results of the 4 × 400 LIS, with several numbers of users, and with different receiver types.

5. Conclusions

This work introduces a neural-network-based approach for interference cancellation in LIS systems employing MRC and EGC receivers. The proposed method replaces traditional iterative interference cancellation techniques by leveraging an MLP to estimate

the transmitted signals directly from the output of a single-iteration MRC/EGC receiver, which comprises interference-corrupted signals. This approach effectively mitigates the interference generated in the decoding process of MRC/EGC, improving signal recovery without requiring explicit channel matrix inversion, as required for ZF and MMSE receivers. Moreover, it is observed that the MRC/EGC neural network outperforms MMSE and ZF. Finally, it is observed that the MRC always outperforms EGC (with or without a neural network).

The chosen network architecture, consisting of three fully connected layers with ReLU activation, is selected based on extensive empirical evaluations, balancing complexity and performance. A deeper network does not yield significant improvements, while a shallower one results in a degraded performance. The simulation results demonstrate that the proposed neural-network-based approach outperforms traditional iterative interference cancellation methods in terms of signal reconstruction accuracy while maintaining computational efficiency. The decision to train separate neural networks per transmit antenna is justified by the statistical independence of antennas, ensuring robustness against varying channel conditions. Additionally, alternative architectures such as CNNs and LSTM networks are considered, but are deemed less suitable due to the absence of strong spatial or temporal dependencies in the interference structure.

Overall, this work confirms that neural networks provide a promising alternative for interference mitigation in LIS receivers, offering a practical and scalable solution for future 6G communication systems.

Future work could explore deeper neural architectures and test the proposed approach in real-time scenarios to validate its practical applicability. Moreover, although this work focuses on comparing neural-network-based receivers with conventional MRC, EGC, ZF, and MMSE techniques, future work will also consider iterative ZF/MMSE approximations that avoid matrix inversion, such as those based on the Jacobi, Newton, or Neumann methods, as part of a broader comparative study.

Author Contributions: Research and numerical analysis was carried out by the first author, whereas the other authors supported conceptualization. All authors have read and agreed to the published version of the manuscript.

Funding: This work is funded by FCT/MECI through national funds and when applicable co-funded EU funds under UID/50008: Instituto de Telecomunicações.

Data Availability Statement: Monte Carlo simulations were performed using MATLAB R2025a to obtain the data presented.

Acknowledgments: The authors acknowledge the support of FCT/MCTES (as detailed in the Funding Section) and Autonoma TechLab for providing a stimulating research environment.

Conflicts of Interest: The authors declare no conflicts of interest.

References

1. Kunze, L.; Hawes, N.; Duckett, T.; Hanheide, M.; Krajnik, T. Artificial Intelligence for Long-Term Robot Autonomy: A Survey. *IEEE Robot. Autom. Lett.* **2018**, *3*, 4023–4030. [CrossRef]
2. Mariani, M. Big IoT Data Analytics: Architecture, Opportunities, and Open Research Challenges. *IEEE Access* **2017**, *5*, 5247–5261.
3. Cabeças, A.; Marques da Silva, M. Project Management in the Fourth Industrial Revolution. *TECHNO REVIEW Int. Technol. Sci. Soc. Rev.* **2021**, *9*, 79–96. [CrossRef]
4. Mu, X.; Xu, J.; Liu, Y.; Hanzo, L. RIS-Aided Near-field Communications for 6G: Opportunities and Challenges. *arXiv* **2023**, arXiv:2312.13004.
5. Decarli, N.; Dardari, D. Communication Modes with Large Intelligent Surfaces in the Near Field. *IEEE Access* **2021**, *9*, 165648–165666. [CrossRef]

6. Bjornson, E.; Özlem, T.; Sanguinetti, L. A primer on near-field beamforming for arrays and reconfigurable intelligent surfaces. In Proceedings of the 2021 55th Asilomar Conference on Signals, Systems, and Computers (ACSSC), Pacific Grove, CA, USA, 31 October–3 November 2021; pp. 105–112.
7. Marques da Silva, M.; Gashtasbi, A.; Dinis, R.; Pembele, G.; Correia, A.; Guerreiro, J. On the Performance of Partial LIS for 6G Systems. *Electronics* **2024**, *13*, 1035. [CrossRef]
8. Gashtasbi, A.; Marques da Silva, M.; Dinis, R. IRS, LIS, and Radio Stripes-Aided Wireless Communications: A Tutorial. *Appl. Sci.* **2022**, *12*, 12696. [CrossRef]
9. Li, S.; Yang, R.; Guo, X.; Han, G.; Zhang, J. Parametric channel estimation for RIS-assisted mmWave MIMO-OFDM systems with low pilot overhead. *Signal Process.* **2024**, *225*, 109611. [CrossRef]
10. Li, S.; Lei, H.; Dong, Z.; Yang, R.; Guo, X. Two-Stage Channel Estimation in mmWave MIMO Systems with RIS Blockage. *IEEE Wirel. Commun. Lett.* **2024**, *13*, 3548–3552. [CrossRef]
11. Dajer, M.; Ma, Z.; Piazzi, L.; Narayan, P.; Qi, X.; Sheen, B.; Yang, J.; Yue, G. Reconfigurable Intelligent Surface: Design the Channel—A New Opportunity for Future Wireless Networks. *arXiv* **2020**, arXiv:2010.07408v1. [CrossRef]
12. Gashtasbi, A.; Marques da Silva, M.; Dinis, R.; Guerreiro, J. On the Performance of LDPC-Coded Large Intelligent Antenna System. *Appl. Sci.* **2023**, *13*, 4738. [CrossRef]
13. Farsad, N.; Goldsmith, A. Detection Algorithms for Communication Systems Using Deep Learning. In Proceedings of the 31st Conference on Neural Information Processing Systems (NeurIPS 2017), Long Beach, CA, USA, 4–9 December 2017.
14. Xu, W.; Zhong, Z.; Be'ery, Y.; You, X.; Zhang, C. Joint Neural Network Equalizer and Decoder. In Proceedings of the 2018 International Symposium on Wireless Communication Systems (ISWCS), Lisbon, Portugal, 28–31 August 2018; pp. 1–6. [CrossRef]
15. Hu, S.; Rusek, F.; Edfors, O. Beyond Massive-MIMO: The Potential of Data-Transmission with Large Intelligent Surfaces. *arXiv* **2017**, arXiv:1707.02887v1. [CrossRef]
16. Pavia, J.P.; Velez, V.; Souto, N.; Marques da Silva, M.; Correia, A. System-Level Assessment of Massive Multiple-Input–Multiple-Output and Reconfigurable Intelligent Surfaces in Centralized Radio Access Network and IoT Scenarios in Sub-6 GHz, mm-Wave, and THz Bands. *Appl. Sci.* **2024**, *14*, 1098. [CrossRef]
17. Borger, D.; Dinis, R.; Montezuma, P. An MRC-Based Receiver for SC-FDE Modulations with Massive MIMO Schemes. In Proceedings of the 2016 IEEE Global Conference on Signal and Information Processing (Global SIP), Washington, DC, USA, 7–9 December 2016.
18. Marques da Silva, M.; Dinis, R.; Guerriero, J. A Low Complexity Channel Estimation and Detection for Massive MIMO using SC-FDE. *Telecom* **2020**, *1*, 3–17. [CrossRef]
19. Marques da Silva, M.; Dinis, R.; Aleixo, J.; Oliveira, L.M.L. On the Performance of LDPC-Coded MIMO Schemes for Underwater Communications Using 5G-like Processing. *Appl. Sci.* **2022**, *12*, 5549. [CrossRef]
20. Marques da Silva, M.; Dinis, R.; Martins, G. On the Performance of LDPC-Coded Massive MIMO Schemes with Power-Ordered NOMA Techniques. *Appl. Sci.* **2021**, *11*, 8684. [CrossRef]
21. Wang, J.; Baykas, T.; Funada, R.; Sum, C.S.; Rahman, A.; Lan, Z.; Harada, H.; Kato, S. A SNR Mapping Scheme for ZF/MMSE Based SC-FDE Structured WPANs. In Proceedings of the VTC Spring 2009—IEEE 69th Vehicular Technology Conference, Barcelona, Spain, 26–29 April 2009.
22. Montezuma, P.; Borges, D.; Dinis, R. Low Complexity MRC and EGC Based Receivers for SC-FDE Modulations with Massive MIMO Schemes. In Proceedings of the IEEE Global Conference on Signal and Information Processing-Global SIP, Washington, DC, USA, 7–9 December 2016.